

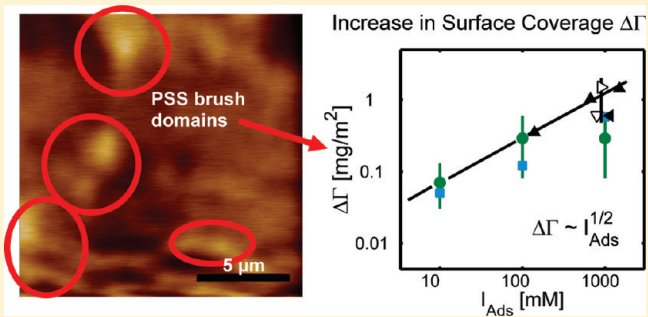
Equilibrium and Nonequilibrium Features in the Morphology and Structure of Physisorbed Polyelectrolyte Layers

Stephan Block* and Christiane A. Helm

Institut für Physik, Ernst-Moritz-Arndt Universität, Felix-Hausdorff-Strasse 6, D-17489 Greifswald, Germany

Supporting Information

ABSTRACT: AFM is used to characterize sodium poly(styrene sulfonate) (PSS) layers physisorbed from NaCl solutions with an ionic strength ranging between 0 and 1 M NaCl. Colloidal probe tapping mode imaging shows that domains of PSS salted brushes coexist with flatly adsorbed PSS. The brush area fraction increases with rising degree of polymerization. The surface forces (as measured with colloidal probe technique) are a superposition of steric and electrostatic forces; their respective contribution is determined by the brush area fraction. Unexpectedly, the internal properties of the brush domains (brush thickness and average chain distance) are independent of the deposition salt concentration. Both properties increase with rising polymer length/degree of polymerization, whereas only the brush thickness can be controlled by the surrounding salt concentration (equilibrium feature). Furthermore, we show that the amount of brush-like physisorbed PSS chains leads to an increase in PSS surface coverage, which is also observed with other techniques after addition of salt to the deposition solution (as is extensively described in literature).



INTRODUCTION

Adsorbed polyelectrolytes (PEs) are used in a multitude of traditional applications (for example as wet and dry strength additives) but also in basic research in connection with material and the life sciences.^{1–5} In these fields one often takes advantage of the fact that polyelectrolytes bear ionizable groups (incorporated within the monomeric units) which can be charged in aqueous solutions and which lead to a strong affinity toward oppositely charged surfaces.

In order to understand and optimize the properties of adsorbed polyelectrolytes for the desired application, many theoretical and experimental efforts have been performed in the past years.^{6–10} In this context the direct measurement of surface forces arising between polyelectrolyte covered surfaces proved to be a very powerful technique for the investigation of adsorbed polyelectrolyte layers.^{11–13} For example, it is well established that the dominant force between two flat surfaces (of equal charge) is given by the repulsive electrostatic double layer force which can be measured with high precision using the surface forces apparatus (SFA) or the colloidal probe technique (CPT).^{14–19}

Generally, the adsorption of single polyelectrolyte layers changes the interactions between the surfaces.^{15,20} For polyelectrolytes adsorbed from salt free solution, one often observes a mixture of short ranged attraction (commonly attributed to van der Waals forces or patch charge attraction) and longer ranged double layer repulsion which indicates that the polyelectrolytes adsorb in a rather flat conformation.^{11,21–25} Furthermore, measurements indicate that most of the adsorbed polyelectrolyte is

usually confined in a thin layer with a thickness of a few nanometers which is completely in agreement with theoretical considerations and attributed to the strong electrostatic attraction acting between the monomers and the surface charges.^{6,25–31}

However, the addition of salt to the adsorption solution has often a profound effect on the conformation of adsorbed polyelectrolytes, and hence, the measured force profile can be very different from flatly adsorbed polyelectrolytes (adsorption from salt-free solution). For example, in their pioneering work Luckham and Klein were able to show that the addition of 0.1 M KNO₃ to the salt solution changes the force profiles between poly-L-lysine covered mica surfaces from pure electrostatics to long ranged steric forces which indicates, that (at least) some of the PE chains adsorb in a nonflat conformation onto the surface.³²

On the basis of this work and using CPT, we investigated several linear PEs and found that this nonflat conformation (observed after adsorption from solutions containing 1 M NaCl) is very similar to that of polyelectrolyte brushes: the thickness of the physisorbed PE layer scales like a salted polyelectrolyte brush and reaches up to 1/3 of the contour length (on decrease of the surrounding salt concentration).^{33–36} Interestingly, the surface forces acting between such layers are well described by the theory of Alexander and de Gennes which was originally derived for anchored neutral polymer brushes and which allows an easy

Received: December 21, 2010

Revised: April 28, 2011

Published: May 17, 2011

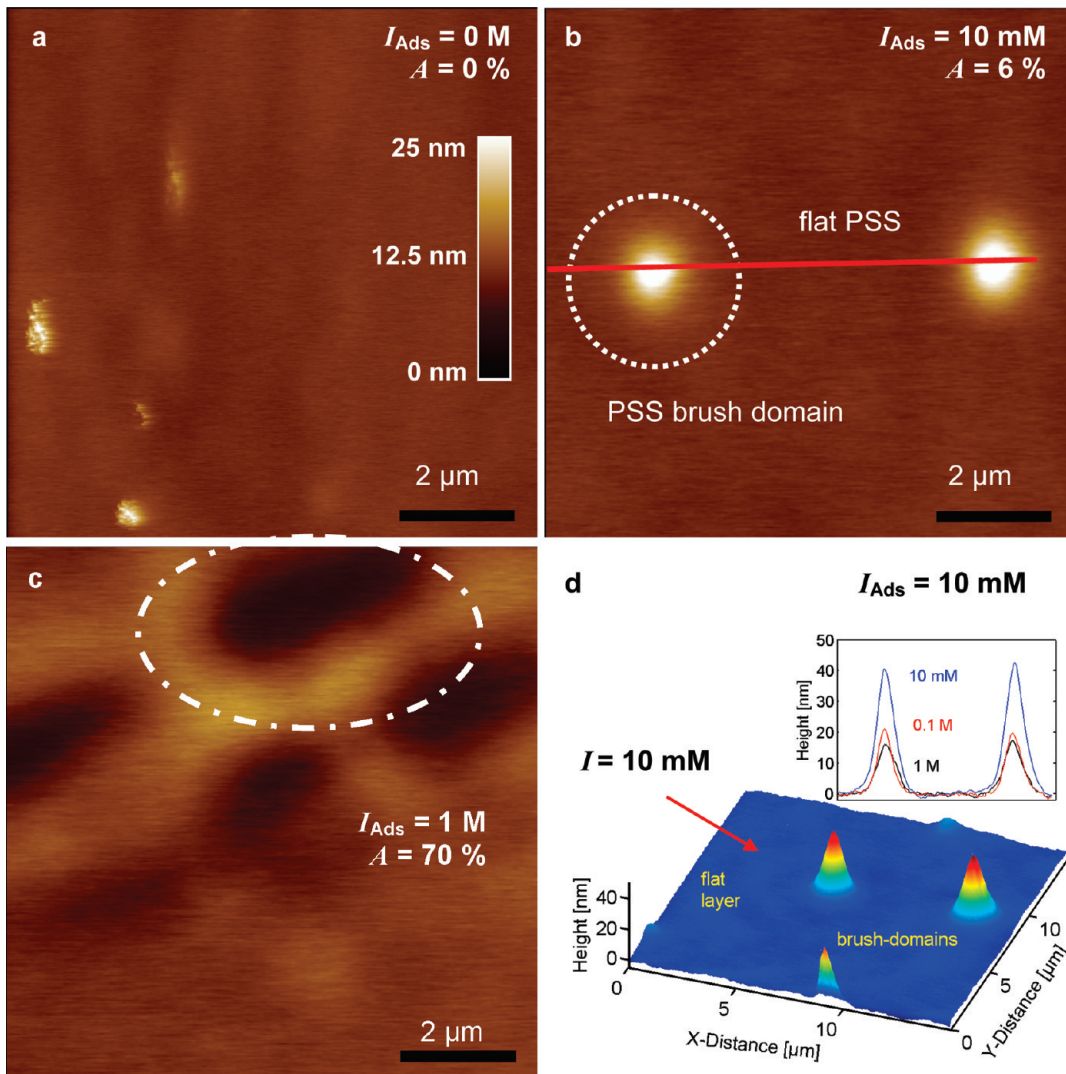


Figure 1. Colloidal probe tapping mode (CPTM) images of the PSS layer: degree of polymerization $N = 840$; adsorbed at I_{AdS} as indicated; measured at $I = 0.1 \text{ M}$ (a–c) or as indicated in the inset (d), respectively; scale bar = $2 \mu\text{m}$; z-range = 25 nm ; also given is the area fraction A of the brush domains (see text); panels b and d show the same sample. (a) For adsorption from salt free solution ($I_{\text{AdS}} = 0 \text{ M NaCl}$) flatly adsorbed PSS chains are found as expected (the structures on the left side of the image can be related to impurities on the surfaces, see text). (b) After adsorption from a solution containing $I_{\text{AdS}} = 10 \text{ mM NaCl}$ islands are observed (dotted circle) which can be attributed to PSS chains in a PE brush-like conformation (cf. swelling/shrinking experiments shown in d) and shows that PSS adsorbs in (at least) two phases even at rather small salt concentrations. A further increase of I_{AdS} to 1 M NaCl (c) leads to almost full coverage of the brush phase, and hence, holes (dash-dotted circle) are imaged within a thick PSS layer.

quantification of the internal properties of the adsorbed PE brush (grafting density and equilibrium brush thickness).^{37,38}

Recently, it was shown for sodium poly(styrene sulfonate) (PSS) physisorbed from 1 M NaCl that the amount of brush-like physisorbed PE chains depends strongly on the degree of polymerization N of the PSS: For $N \geq 1100$ the whole surface is covered by the brush-like adsorbed PSS, whereas for $N < 1100$ a coexistence of domains of flatly and brush-like adsorbed PSS is found.³⁹ Conveniently, both PSS phases can be distinguished by tapping mode imaging in liquid (cf. Figure 1), if a CP instead of a sharp tip is used (which avoids the penetration of the tip into the brush).^{36,40} Hence, the surface coverage of the PSS brush domains can be easily determined.

These observations show that in absence of salt polyelectrolytes usually adsorb in a rather flat and compact layer onto an oppositely charged surface, whereas the addition of salt promotes

the adsorption of linear polyelectrolytes in nonflat conformations. This behavior can be qualitatively understood if one keeps in mind that in the salt-free case linear polyelectrolytes already exhibit a rather stretched conformation (due to the strong electrostatic monomer–monomer repulsion), whereas high amounts of salt in the bulk phase effectively screen the electrostatic interaction which leads to a highly coiled chain conformation within the adsorption solution.⁴¹ Obviously, a flat and compact adsorption of a coiled chain requires a strong confinement and is therefore entropically not preferred.

However, it is well-known that the electrostatic stiffening of linear PE chains can be continuously controlled by the salt concentration.⁴¹ Hence, if it is possible to achieve a continuous transition between a coiled and a stretched conformation in solution, the question automatically arises what kind of chain conformation will be found after adsorption onto a surface.

Here, we address this question by resolving the surface properties of sodium poly(styrene-sulfonate) (PSS) layers formed after adsorption onto silanized silica substrates (the silane has a positively charged end-group, for experimental details please refer to the Materials and Methods section). By adding sodium chloride salt (concentration I_{Ads}) to the adsorption solution we are able to choose a conformation of the linear polyelectrolyte which is between a rather stretched ($I_{\text{Ads}} = 0 \text{ M}$) or a highly coiled ($I_{\text{Ads}} = 1 \text{ M NaCl}$) state.^{42,43} Using colloidal probe tapping mode (CPTM) we are able to image the domains of the PSS brush phase (in dependence on I_{Ads} and the degree of polymerization N) and therefore to study the spatial properties of these domains. By connecting the measurements of CPTM with direct force measurements (performed using colloidal probe technique, CPT) we characterize the internal properties of the brush phase and we derive the scaling laws for brush thickness L , average chain distance s and brush area fraction A with respect to I_{Ads} and N . Finally, by combining this information, we are able to estimate the amount of brush-like physisorbed PSS chains and to relate this value to the increase in surface coverage of physisorbed polyelectrolytes which is usually observed if salt is added to the deposition solution.⁴⁴ The experiments described in literature suggest a close relation between the amount of physisorbed polyelectrolyte and its conformation on the surface.

MATERIALS AND METHODS

All solutions are created with ultrapure water using a Milli-Q device (Millipore, Billerica, MA). Sodium chloride (NaCl, p.a. grade) was obtained from Merck (Darmstadt, Germany) and 3-aminopropyltrimethoxysilane from ABCR (Karlsruhe, Germany). Sodium poly(styrene sulfonate) (PSS) with monomer count ranging from $N = 380$ (contour length $L_C = 95 \text{ nm}$) to 1800 ($L_C = 450 \text{ nm}$) was purchased from Polymer Standard Service (Mainz, Germany) in the following batches: pss13030 (77 kDa, $N = 380$, PDI < 1.1), pss14061 (123 kDa, $N = 600$, PDI < 1.2), pss26058 (168 kDa, $N = 840$, PDI < 1.2), and pss200203 (350 kDa, $N = 1800$, PDI < 1.2). PSS with an average mass of 1.4 MDa ($N = 6800$, $L_C = 1700 \text{ nm}$, PDI < 1.2) was a generous gift of BASF (Ludwigshafen, Germany).

All chemicals are used without further purification. The PSS deposition solutions are prepared by solving 3 mM PSS (with respect to the monomer concentration) in Milli-Q water and by adding NaCl afterward, until the desired ionic strength I_{Ads} (ranging between 0 and 1 M NaCl) is reached.

Colloidal probes (CP) are created by gluing silica spheres (from Bangs Laboratories, Fishers, IN; radius $R \approx 3 \mu\text{m}$, determined using an optical microscope) with UV-curable epoxy (NOA68, Norland Adhesives, Cranbury, NJ) onto the following cantilevers: for colloidal probe tapping mode (CPTM) cantilevers NP-0 (spring constant $k = 0.58 \text{ N/m}$) from Veeco (Dourdan, France); for Colloidal Probe Technique (CPT) cantilevers CSC12 (spring constant $k = 0.005$ to 0.03 N/m) from MicroMasch (Tallinn, Estonia).^{18,19,35}

Surface Preparation. Microscope slides (Roth, Karlsruhe, Germany) are used as silica surfaces. They are cleaned according to the RCA standard and freshly used. CPs are cleaned with argon-plasma at 35 W for 2 min (Harrick Scientific, NY). The surfaces (intended for PSS adsorption) are positively charged by silanization (one day in argon-silane atmosphere, direct use after silanization) and coated with PSS by physisorption from NaCl solution (with ionic strength I_{Ads} between 0 and 1 M NaCl) for

1 h at 30 °C. After adsorption the surfaces are directly transferred (that is without drying) into the fluid cell of our commercial DI Multimode AFM with Nanoscope IIIa Controller (Santa Barbara, CA). For asymmetric measurements and imaging bare CPs are cleaned with argon-plasma at 35 W for 2 min and directly used.

Force Measurements. The force measurements are performed after PSS adsorption in NaCl solutions (free of PSS) of different ionic strengths I : starting at 0.1 M, then diluting down to 1 mM and enriching again to 0.1 M. Force curves are recorded not later than five minutes after change of the solution. We perform symmetric measurements (both surfaces covered with PSS) as well as asymmetric measurements (one PSS covered surface against a bare silica CP or a silicon tip). During one experiment we record at least 200 force curves for each salt concentration at different positions on the surface, with one approach/separation cycle per five seconds. Shown are only the averaged force curves. After the measurement spring constants are determined using the methods of Butt, Sader and Cleveland.^{45–47} All in all, more than 60 000 force curves were recorded.

Afterward, the distance dependent force curves $F(D)$ are normalized by the radius of the CP to give (according to Derjaguin's approximation) the interaction energy per unit area $W(D)$ of two flat surfaces: $W(D) = F(D)/(2\pi R)$.⁴⁸ This allows an easy quantification of the force curves with the theoretical models which are often calculated for the interaction of two infinitely extended flat surfaces.

Imaging. The morphology of the PSS layers is measured using AFM colloidal probe tapping mode (CPTM) in PSS free NaCl solutions of different ionic strengths I (between 1 M and 1 mM NaCl as indicated) as described previously.³⁵ In this study 512 × 512 pixels are recorded per image and the z-limit of the piezo scanner was set to 500 nm, in order to increase the height resolution of the AFM. Directly after preparation (of the CP) CPTM images with a coarse lateral resolution (curvature radius = CP radius $R = 3 \mu\text{m}$) are obtained.

Image Processing. Images obtained with the AFM are stored in raw data format, that is in absence of any automated filtering or image processing by the AFM software. Afterward, the images are processed using the Nanoscope 5 software (which is delivered with our commercial DI Multimode AFM) as follows: For larger images (scan area $> 1 \times 1 \mu\text{m}^2$) the spherical distortion introduced by the piezo scanner is removed by fitting a spherical plane (of second order) into the data and by subtracting the fitted spherical plane from the data. For smaller images this correction is skipped, as no distortion was noticeable.

Reproducibility. All measurements (CPT and imaging) are repeated at least twice with freshly prepared surfaces.

RESULTS

Surface Morphology for PSS Physisorbed at Different I_{Ads} . The morphology of the physisorbed PSS layers is investigated using colloidal probe tapping mode (CPTM) as described previously.³⁵ Here, the use of a bare colloidal probe (CP) instead of a sharp tip increases the contact area and hence the interaction between the cantilever and the PSS chains protruding into solution can be estimated during imaging. Figure 1 shows a representative example of the morphology of single PSS layers ($N = 840$) which are physisorbed from a deposition solution of different NaCl salt concentration I_{Ads} and which are imaged at a bulk salt concentration $I = 0.1 \text{ M NaCl}$. (Please note that in the following two different salt concentrations are generally

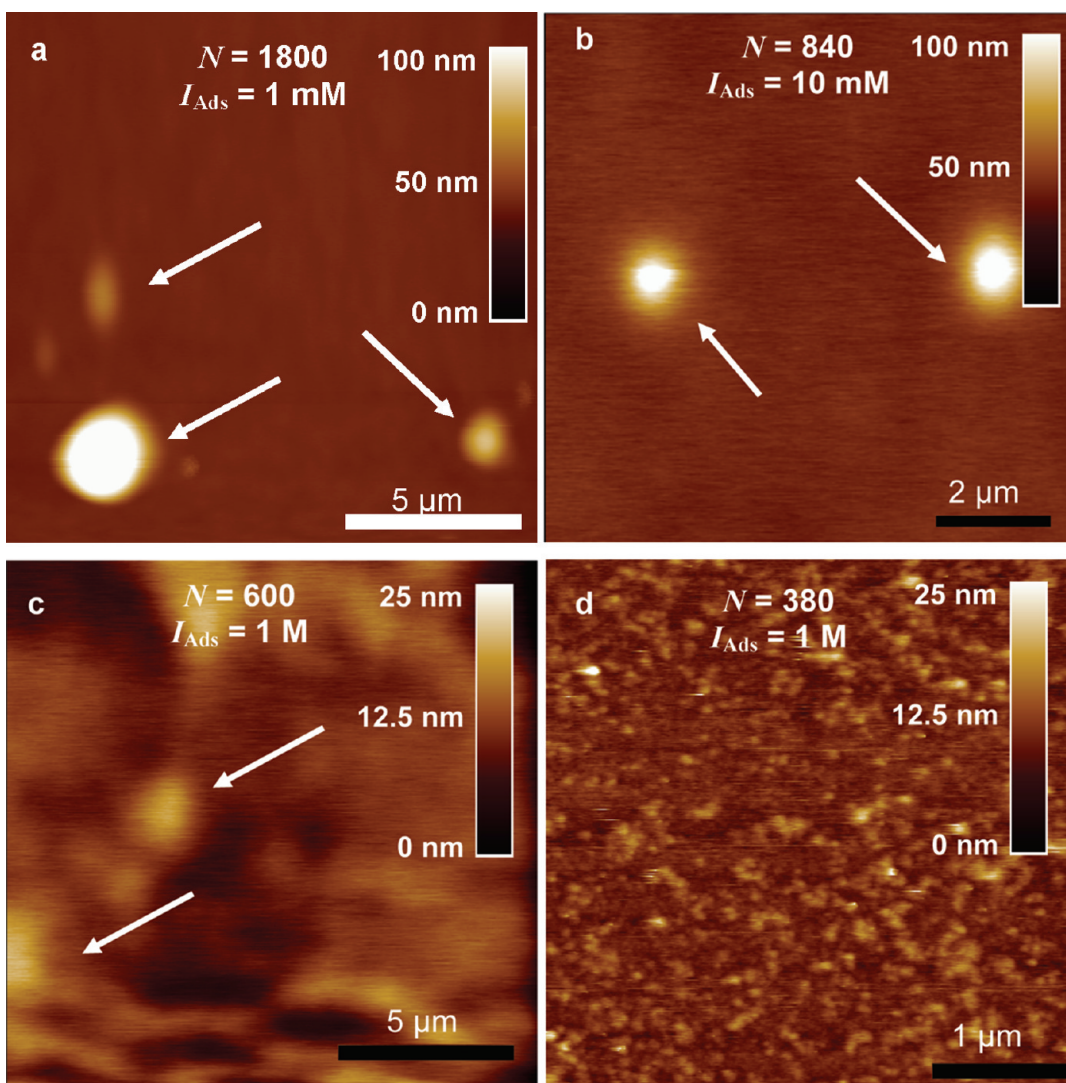


Figure 2. Colloidal probe tapping mode (CPTM) images of PSS layers, imaged at a surrounding salt concentration $I = 1 \text{ mM NaCl}$. Each figure corresponds to a different degree of polymerization N (as indicated). The deposition salt concentration I_{Ads} was adjusted that for all values of N a coexistence of flat and nonflat/PSS brush domains (white arrows) can be observed. Hence, a heterogeneous morphology of physisorbed PSS layer is a general feature, which can be controlled by choosing the appropriate values for N and I_{Ads} . (Please note the different length and height scales, which can be inferred from the scale and color bars. For panels a to c, a colloidal probe with $R \approx 3 \mu\text{m}$ was used, while in panel d the sample is inspected by a tip with $R \approx 100 \text{ nm}$.)

considered: I_{Ads} refers to the NaCl concentration in the deposition solution and determines the PSS conformation and surface properties during the adsorption process. In contrast to this, the NaCl concentration during the CP and CPTM measurements is denoted by I . Hence, this concentration determines the properties of the physisorbed PSS layer during the measurement. The once formed ionic bonds between the PSS and the surface are not affected by a change of the salt content in the solution in the range between 0 and 1 M NaCl.³⁶

For adsorption from salt free solution ($I_{\text{Ads}} = 0 \text{ M NaCl}$, cf. Figure 1a), flatly adsorbed PSS is observed as expected. There are some structures visible on the left side of the image, which can be related to impurities on the surfaces: Please note the “increased” lateral resolution of the image at the impurities (sharp features are visible) compared to the rest of the surface. This is a clear indication that these impurities act like spikes in CPTM and therefore a “self imaging” of the CP is observed at these impurities. Furthermore, a change of the surrounding salt concentration I has

no effect on the layer morphology, which shows that the surface is homogeneously covered by flatly adsorbed PSS.

However, the morphology of the physisorbed layer changes dramatically if salt is added to the deposition solution: For $I_{\text{Ads}} = 10 \text{ mM NaCl}$ (cf. Figure 1b) islands are observed which exhibit a height on the order of several 10 nm (cf. Figure 1d) and which are subject to swelling (or shrinking) if the bulk salt concentration I is decreased (or increased, respectively). On a further increase of the salt content in the deposition solution (for example $I_{\text{Ads}} = 1 \text{ M NaCl}$, see Figure 1c) the “inverted” situation is resolved (holes within an extended PSS layer appear, see dash-dotted circle) which shows that the area fraction of the domains (= area fraction occupied by nonflatly adsorbed PSS) rises by an increase of I_{Ads} .

These examples clearly show that the addition of salt to the deposition solution leads to a nonflat conformation of physisorbed PSS chains. However, measurements performed for different degrees of polymerization N show that this is a general feature, which is found for all N investigated (cf. Figure 2).

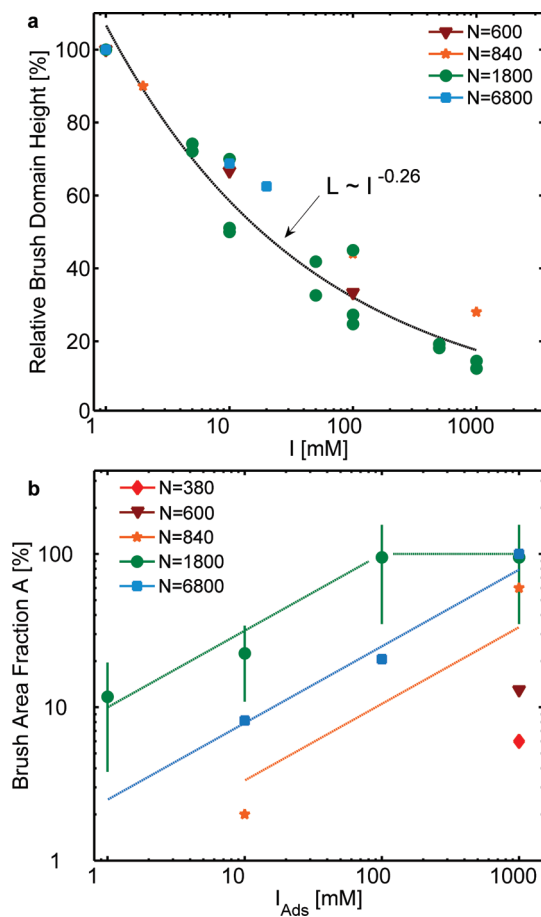


Figure 3. (a) Using CPTM the height $H(I)$ of the brush domains can be easily resolved in dependence of the bulk salt concentration I (the deposition salt concentration I_{AdS} was chosen in such way, that isolated PSS brush domains are resolved by CPTM). However, to investigate the swelling/shrinking behavior of these domains it is more useful to examine the relative height $h(I)$, which is simply the ratio between the height at I and its value at $I = 1 \text{ mM}$ (cf. text). Interestingly, CPTM reveals that the height of the domains generally scales with the power law $I^{-0.26}$, which is close to $I^{-1/3}$ expected for polyelectrolyte brushes. (b) Additionally, due to the swelling behavior it is easy to determine the area fraction A of the brush domains (area occupied by brush-like adsorbed PSS chains per unit area). There is a monotonic increase in A with rising I_{AdS} , which appears to scale like $A \sim (I_{\text{AdS}})^{1/2}$, while the dependence on N is nonmonotonic and not so trivial (cf. text).

Furthermore, the height of these domains (of nonflatly physisorbed PSS chains) is on the order of several 10 nm for all N and strongly depends (like in Figure 1, panels b and d) on the bulk salt concentration I . Hence, it is concluded (like in previously performed measurements) that the nonflat physisorbed PSS chains exhibit a brush-like conformation.³⁹ Therefore, we conclude that the domains observed in CPTM are PSS brush domains.

If this assumption is correct, the height H of the brush domains should scale with the ionic strength I of the surrounding solution like a salted polyelectrolyte brush: $H \sim I^{-1/3}$.³³ Figure 3a shows this dependence for the relative height $h(I) = H(I)/H(1 \text{ mM})$ of the domains, that is the ratio of the domain height $H(I)$ measured at I normalized to the domain height $H(1 \text{ mM})$ at 1 mM. This normalization is necessary as longer PSS chains (that is larger N) usually generate higher brush domains (see the Supporting Information) and hence the normalization

allows an easy comparison of the swelling/shrinking behavior of PSS chains which differ in N .

Figure 3a shows that the brush domains generally swell (shrink) with an increase (decrease) in I . Furthermore, the data points can be well explained by the power law $I^{-0.26}$, which is close to $I^{-1/3}$ expected for polyelectrolyte brushes. Again, these islands can be clearly identified as PSS brush domains,³⁹ which surprisingly shows that even a small amount of salt in the deposition solution (for example $I_{\text{AdS}} = 10 \text{ mM NaCl}$ for $N = 840$) leads to the formation of the nonflat PSS brush phase.

Furthermore, this swelling behavior allows an easy determination of the area fraction A of the brush domains: CPTM images are recorded at the same surface position for different I and the areas on the surface, which are subject to strong swelling/shrinking can be easily identified as PSS brush domain (see Figure 1b, d). Figure 3b shows the dependence of A on the degree of polymerization N and the salt concentration I_{AdS} in the deposition solution. In this plot one clearly resolves a monotonic increase of A with rising I_{AdS} , which appears to scale like $A \sim (I_{\text{AdS}})^{1/2}$ (lines in Figure 3b). To the best of our knowledge, there exists at the moment no theoretical explanation for this special scaling, but it very strongly reminds us of the observation that the surface coverage Γ of physisorbed polyelectrolytes often increases with $\Gamma \sim (I_{\text{AdS}})^{1/2}$.^{44,49-56}

However, Figure 3b also shows that the dependence of N on A is nonmonotonic and nontrivial: for a given I_{AdS} the highest brush surface coverage is found for $N \approx 1800$ and both increasing and decreasing N leads to a decrease in A . This shows that ratio between flat and nonflat physisorbed PSS chains does not only depend on I_{AdS} but also strongly on the length of the PSS chain.

Additionally, it was shown previously that for chains, which are strongly coiled in the deposition solution (low persistence length compared to the contour length), the nonflat adsorption can be understood in terms of a gain in entropy:³⁹ If flatly physisorbed chains are replaced by nonflat ones, the conformational freedom per chain increases and hence under certain circumstances also the entropy per unit area. The gain in entropy increases with the degree of polymerization N , and hence, longer chains prefer to physisorb in a nonflat conformation. However, the dependence on N in Figure 3b clearly shows that this image is too simple and has to be extended for chains whose conformation in solution is in between a fully stretched or coiled state, respectively.

Quantification of the Surface Force Caused by Inhomogeneously Physisorbed PSS Layers. To gain more information about the internal properties of the PSS brush domains (prepared at different values of I_{AdS} and N) measurements are performed in order to resolve the distance dependent surface force $F(D)$ created by physisorbed PSS layers. Obviously, from the CPTM images and Figure 3b, one can infer that the layers are generally inhomogeneous: PSS domains containing chains of flat or nonflat conformations coexist, respectively. However, each PSS phase creates its unique surface force and hence for a quantitative investigation of the surface forces one first has to calculate the surface force which is caused by an inhomogeneously physisorbed PSS layer.

From force measurements performed on flatly physisorbed PSS ($A = 0$) it is well-known that the surface force is dominated by an electrostatic double layer repulsion which is independent of N .^{15,25,36,57} The origin of this force can be found in the overlap of counterion clouds which form in the vicinity of charged surfaces (with surface charge σ or surface potential ψ_0 , respectively).⁵⁸ If two equally charged surfaces approach, an excess osmotic

pressure will arise (due to the overlap of counterion clouds) which leads to a repulsive force acting on both surfaces.

It can be shown that for monovalent salts, at surface separations D larger than the Debye length κ^{-1} ($= 0.304 \text{ nm}/(I)^{1/2}$) and for surface potentials $\psi_{0,1/2} < 25 \text{ mV}$ the electrostatic repulsion is well described by

$$\frac{F_{\text{DL}}(D)}{2\pi R} = 0.0482\sqrt{I} \tanh\left[\frac{\psi_{0,1}}{103 \text{ mV}}\right] \tanh\left[\frac{\psi_{0,2}}{103 \text{ mV}}\right] e^{-\kappa D} \quad (1)$$

where $\psi_{0,1/2}$ denotes the respective surface potential at infinite surface separation.¹⁵

However, for homogeneous layers of brush-like physisorbed PSS chains it was shown that the distance dependent surface forces are very well described by the theory of Alexander and de Gennes.^{35,36,39} De Gennes extended the theory of Alexander to describe the steric force acting between two end-grafted neutral polymer-brushes (called AdG theory below)^{37,38,39} and calculated an interaction energy per unit area of two brushes (of thickness L and grafting density $\Gamma = s^{-2}$) of

$$\frac{F_{\text{AdG,symm}}(D)}{2\pi R} = \frac{8k_B TL}{35s^3} \left[7\left(\frac{2L}{D}\right)^{5/4} + 5\left(\frac{D}{2L}\right)^{7/4} - 12 \right] \text{ for } D < 2L \quad (2)$$

O'Shea et al. used the assumed lack of brush interpenetration to show that this theory can be successfully applied to describe the interaction of a polymer brush with a bare, nonadsorbing surface.⁶⁰ They conclude that this asymmetric case can be described with eq 2 by replacing $2L$ by L and dividing eq 2 by 2,¹² leading to

$$\frac{F_{\text{AdG,asymm}}(D)}{2\pi R} = \frac{2k_B TL}{35s^3} \left[7\left(\frac{L}{D}\right)^{5/4} + 5\left(\frac{D}{L}\right)^{7/4} - 12 \right] \text{ for } D < L \quad (3)$$

Throughout this work we will denote the first situation as symmetric case (both surfaces are symmetrically covered by PSS) whereas the second situation will be called asymmetric case (as one bare surface is asymmetrically interacting with one PSS covered surface).

The AdG force profiles are nonlinear functions which can be well approximated at intermediate surface separations ($0.2 \leq D/L \leq 0.9$) by an exponential function with a decay length given by $\gamma^{-1} = -L/\pi$ (symmetric) and $\gamma^{-1} = -L/2\pi$ (asymmetric), respectively, which depends only on the brush thickness L .^{15,61}

These considerations show that flatly physisorbed PSS chains create an electrostatic repulsion $F_{\text{DL}}(D)$ whereas the brush phase shows only a steric force $F_{\text{AdG}}(D)$. Hence, in a first approximation we assume that the surface force caused by inhomogeneous PSS layers will be a superposition of an electrostatic and a steric force whereas the respective contribution depends on the area fraction the corresponding phase occupies on the surface. From the definition of the area fraction A (occupied by the brush phase) we infer that in the asymmetric case the fraction A of the unit area creates the asymmetric steric force $F_{\text{AdG,asymm}}(D)$ and hence the fraction $(1 - A)$ shows the electrostatic force $F_{\text{DL}}(D)$. Thus, the composed asymmetric force profile has the form

$$F(D) = (1 - A)F_{\text{DL}}(D) + AF_{\text{AdG,asymm}}(D) \quad (4)$$

(with $\psi_{0,1} = \psi_{\text{silica}}$ and $\psi_{0,2} = \psi_{\text{PSS}}$ in $F_{\text{DL}}(D)$).³⁹ Furthermore, for the symmetric case the electrostatic, asymmetric steric and symmetric steric forces will contribute with the fractions $(1 - A)^2$, $2A(1 - A)$, and A^2 , respectively, to the composed symmetric force profile

$$F(D) = (1 - A)^2 F_{\text{DL}}(D) + 2 \cdot A \cdot (1 - A) F_{\text{AdG,asymm}}(D) + A^2 F_{\text{AdG,symm}}(D) \quad (5)$$

(with $\psi_{0,1/2} = \psi_{\text{PSS}}$ in $F_{\text{DL}}(D)$).

Please note that, although the composed force profiles contain many parameters, most of them are known, as will be outlined: The area fraction A of the brush phase (which critically determines the composition of the force profile) can be determined independently using CPTM (cf. Figure 1–3). Thus, A is not a free parameter. Additionally, the electrostatic contribution can be also measured independently (for example by using PSS layers which are physisorbed from salt free deposition solutions or by the interaction of a flat PSS layer with a bare CP) and thus the electrostatic parameters are also no free parameters.^{36,57} Obviously, using this procedure only the two steric parameters L and s of the brush phase remain adjustable in the fit of the measured force profiles.

Additionally, previously we compared the symmetric and asymmetric steric force laws (eq 2 and 3) with the measured force profiles and found that both methods lead to the same parameters L and s .³⁶ This means (technically) that a comparison of symmetric and asymmetric force profiles can be used to validate the obtained steric fit parameters and (physically) that PSS chains adsorbed onto silanized silica at 1 M NaCl show a force law which was originally derived for neutral polymer brushes. As we found only a steric force and no significant electrostatic contribution we infer that the PSS brush appeared neutralized by counterion incorporation which is a property quite unique to salted polyelectrolyte (PE) brushes and established theoretically as well as experimentally.^{62–64}

The validation of the steric parameters L and s will be performed as follows: First the asymmetric force profiles are fitted to eq 4 as described previously,^{36,39} that is by taking the surface potentials (of silica and PSS) from independent force measurements, by calculating the Debye length in accordance to the bulk salt concentration I and by using the value for the area fraction A of the brush phase as determined by CPTM. Then, only the brush thickness L and the average distance s between brush-like physisorbed chains remain as free parameters to the fit. Afterward, the surface forces between symmetric PSS layers are measured. Then, all previously determined parameters are inserted into eq 5 (= the expected composed symmetric force profile) and as there are no free parameters in this equation, a comparison of the measured force profile with the predicted one (according to eq 5) becomes possible.

Quantification for $N = 1800$. The results of this procedure are given for $N = 1800$ in Figures 4 to 7. As all force profiles show no approach-retraction hysteresis and no attractive contributions, only the approach part is given (a log-scale is used for the y -axis).

In detail, Figure 4 shows representative asymmetric force profiles acting between a bare CP and a PSS covered silica surface physisorbed at $I_{\text{Ads}} = 1 \text{ mM NaCl}$ and measured at $I = 1 \text{ mM NaCl}$ (Figure 4a) or as indicated (Figure 4b). This figure shows that a superposition of an electrostatic and a steric contribution according to eq 4 gives a good description of the asymmetric force profiles and that the magnitude of both forces becomes

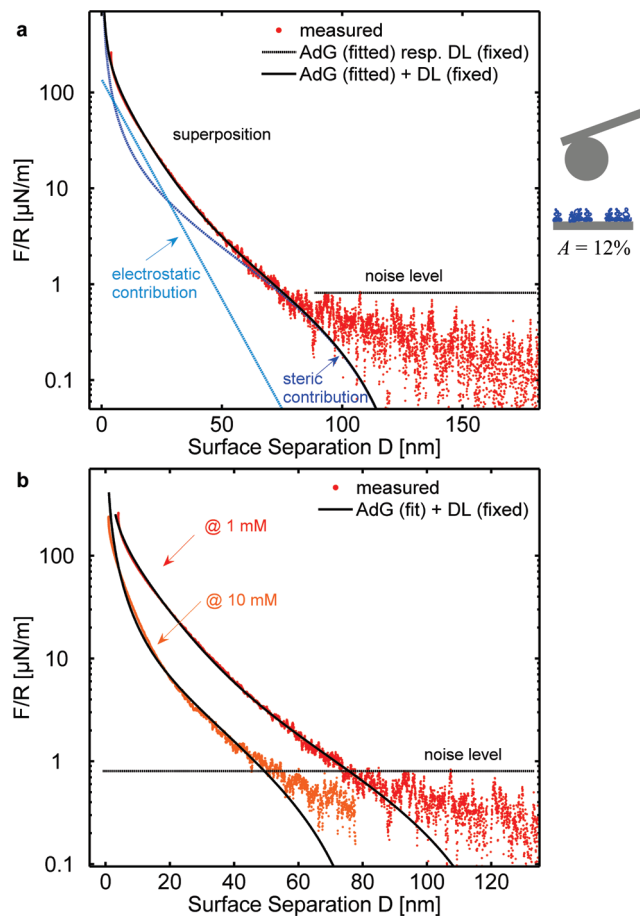


Figure 4. Superposition of an electrostatic and a steric contribution (according to eq 4) gives a good description of the asymmetric force profiles ($N = 1800$, $I_{\text{Ads}} = 1 \text{ mM NaCl}$, asymmetric surfaces setup). Shown are representative force profiles (dots), measured at $I = 1 \text{ mM NaCl}$ (a) or as indicated (b) and the respective fit to eq 4 (dashed blue line: electrostatic and steric contribution, respectively; solid line: superposition).

comparable already at the rather small brush area fraction of 12% for $N = 1800$.

Furthermore, the comparison of the symmetric force profiles predicted by eq 5 with the real measured ones shows that there is a very good agreement of the model with the measured data, although the parameters obtained in the asymmetric case (cf. Figure 4) are used to describe the measurement; no parameter is free/adjustable.

Qualitatively the same is observed in Figures 6 and 7, which show similar measurements performed on PSS layers ($N = 1800$) physisorbed at a larger salt concentration ($I_{\text{Ads}} = 10 \text{ mM NaCl}$) and measured at I indicated. The amplitude of the steric force exceeds the one of the electrostatic one already at an area fraction of 20%. Again, the steric parameters obtained by fits to the asymmetric measurements (cf. Figure 6) can be introduced in eq 5 and lead to a predicted force profile, which is very close to the measured one (cf. Figure 7).

(Please note that the steric parameters, the brush thickness L and the average distance s between brush-like physisorbed chains, are given in Figure 9 and will be discussed after the force profiles for $N = 6800$ have been evaluated.)

Quantification for $N = 6800$. For $N = 6800$ a slightly different picture emerges. First of all, for this degree of polymerization

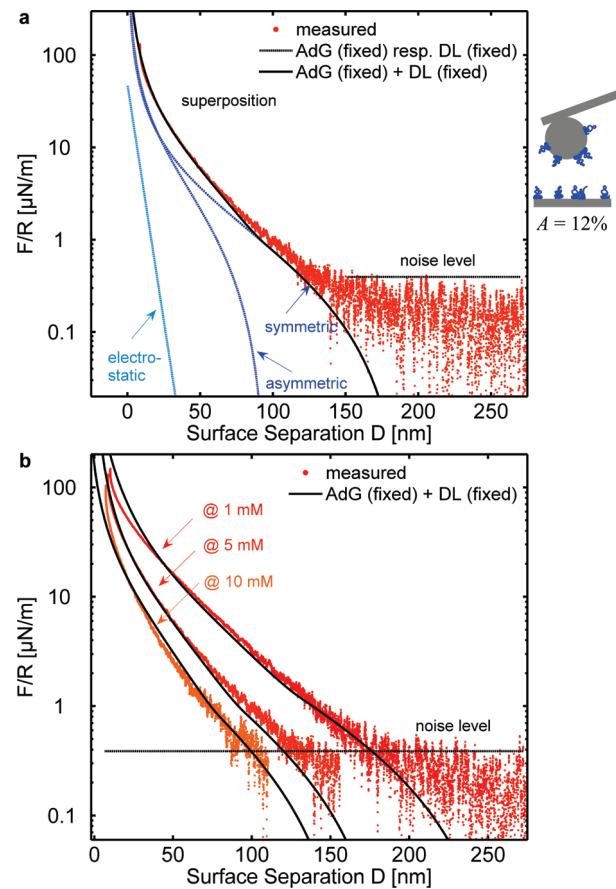


Figure 5. Comparison of the expected symmetric force profiles (solid lines, calculated using eq 5 and the parameters (L, s, A) as obtained by fits of eq 4 to the asymmetric force profiles, cf. Figure 4) with the actual force profiles (dots), measured at $I = 5 \text{ mM NaCl}$ (a) or as indicated (b) ($N = 1800$, $I_{\text{Ads}} = 1 \text{ mM NaCl}$, symmetric surfaces setup). Given are the electrostatic and steric contributions to the force profile (dashed lines), the full superposition (solid line) and the measured data (dots). The good agreement between the predicted and the measured force profiles shows the validity of the model. (Please note that there are no adjustable parameters left.)

even in symmetric surface configuration (both surfaces covered by PSS) only an asymmetric force profile is observed.³⁹ Hence, a test of eqs 4 and 5 as described for $N = 1800$ cannot be performed here, as the symmetric and asymmetric measurements always give very similar force profiles. Therefore, only eq 4 will be applied to obtain the steric parameters. Additionally, the parameters are assumed to be consistent if similar values are determined by fitting eq 4, regardless if there is a symmetric or asymmetric surface setup. (The vanishing of the symmetric contribution in eq 5 is currently not understood and motivates further experiments.)

Furthermore, these samples show additionally a hydrodynamic force contribution to the composed force profile, if a certain approach velocity v_{CP} of the colloidal probe is exceeded (cf. the Supporting Information). This limiting velocity is approximately $v_{\text{CP}} = 1 \mu\text{m s}^{-1}$ for samples physisorbed at $I_{\text{Ads}} = 1 \text{ M NaCl}$ and decreases for smaller values of I_{Ads} . However, systematic measurements on this topic (which will be published separately) reveal that the hydrodynamic force becomes negligible for approach velocities below $v_{\text{CP}} = 0.1 \mu\text{m s}^{-1}$ and hence

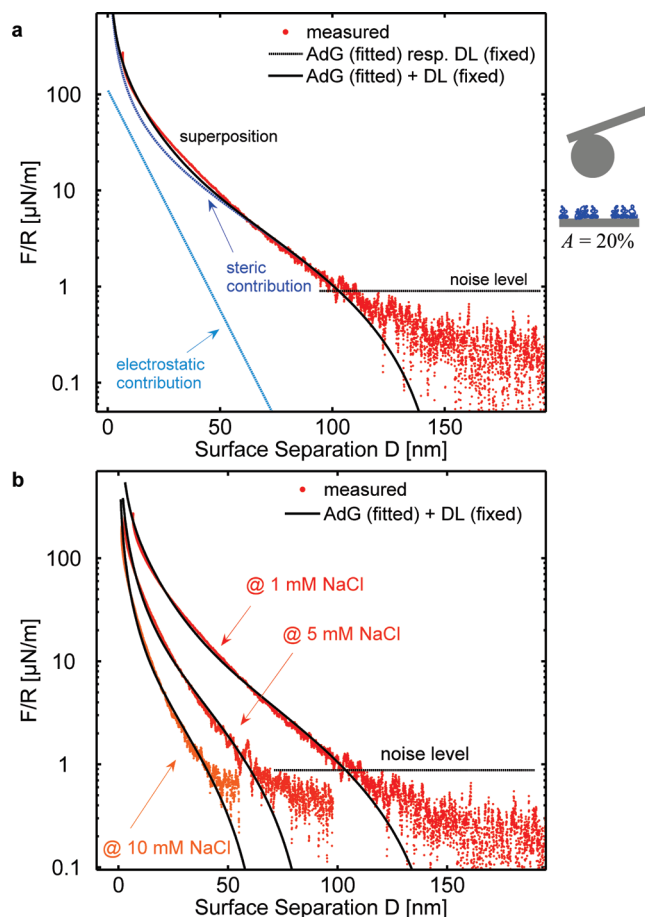


Figure 6. Same as in Figure 4, but for $N = 1800$, $I_{\text{Ads}} = 10 \text{ mM NaCl}$, asymmetric surfaces setup. Again, shown are representative force profiles (dots), measured at $I = 1 \text{ mM NaCl}$ (a) or as indicated (b) and the respective fit to eq 4 (dashed blue line: electrostatic and steric contribution, respectively; solid line: superposition).

all force measurements on PSS with $N = 6800$ have been conducted with this ν_{CP} .

Figure 8 shows the force profiles and the fits to eq 4 (solid lines) for different values of I_{Ads} and I . As before, eq 4 gives a good description of the asymmetric force profiles (please note that the electrostatic contribution can be neglected as its amplitude is very small compared to the steric interaction).

Discussion of the Force Profiles and the Steric Parameters. The force measurements generally show some interesting features:

1. The electrostatic contribution is only noticeable if the steric interaction is small and/or very short-ranged. This is fulfilled for example (i) if the brush area fraction is small (which reduces the magnitude of the steric interaction) or (ii) if short PSS chains are employed. The latter follows from the observation,³⁹ that a decrease of the degree of polymerization decreases also the brush thickness and hence both, the magnitude and range of the steric interaction.
2. On the other hand, the steric interaction is the dominant contribution to the surface forces for large values of the brush area fraction A or brush thickness L . For example, the increase of the salt concentration I_{Ads} from 1 mM to 10 mM NaCl increases the brush area fraction by a factor of approximately 2 for $N = 1800$ (cf. Figure 3b) and hence

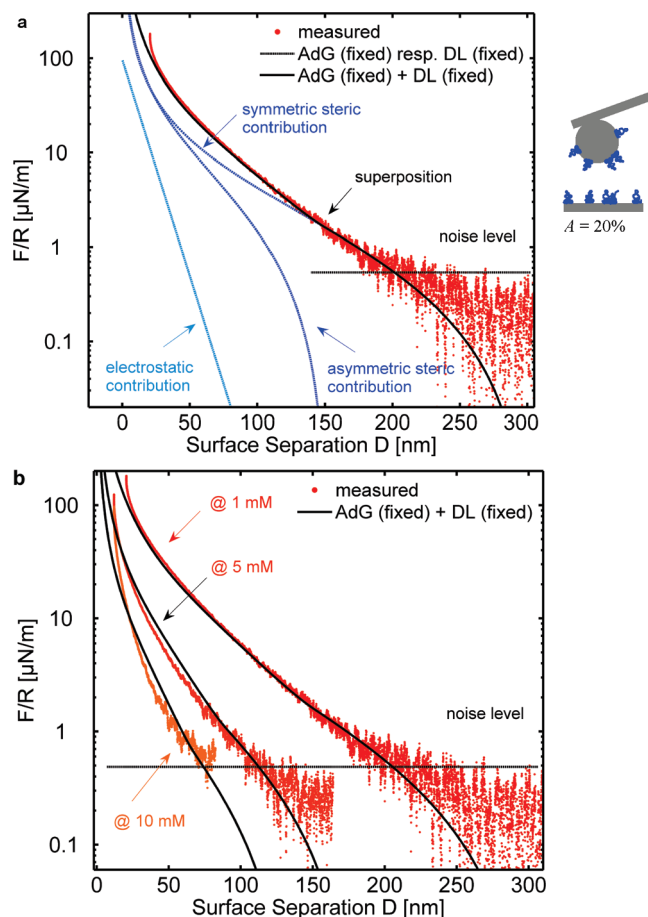


Figure 7. Same as in Figure 5, but for $N = 1800$, $I_{\text{Ads}} = 10 \text{ mM NaCl}$, symmetric surfaces setup. Again, shown are the expected symmetric force profiles (solid lines, calculated using eq 5) and the actual force profiles (dots), measured at $I = 1 \text{ mM NaCl}$ (a) or as indicated (b).

also the magnitude of the steric force is almost doubled (cf. values of $F(D)$ in Figures 4 and 6 at the same surface separation D).

However, a more quantitative picture is obtained if the steric parameters (as obtained by fitting eq 4 to the measured force profiles) are regarded, cf. Figure 9. Here, the full symbols correspond to measurements on PSS layers physisorbed at $I_{\text{Ads}} = 1 \text{ M NaCl}$, whereas open symbols indicate a decrease in I_{Ads} (as indicated in the legends). As in the previous experiments, it is apparent that the average distance s between brush-like physisorbed chains is constant during the measurement, which indicates that there is no rearrangement in the surface upon a change in the bulk salt concentration I .^{36,39} Additionally, the brush thickness L shows again a pronounced dependence on the bulk salt concentration I and scales in agreement with the theory of the salted polyelectrolyte brush.³³

However, within experimental error no dependence of I_{Ads} on the internal properties of the brush phase (s or L) is observed, which is a very surprising result. This means that, although the chain conformation and thus the radius of gyration can be continuously changed between the coiled and stretched state in the deposition solution (by choosing an appropriate I_{Ads}), there is no such continuous transition between flat and nonflat physisorbed PSS. Here, at first sight one would probably expect

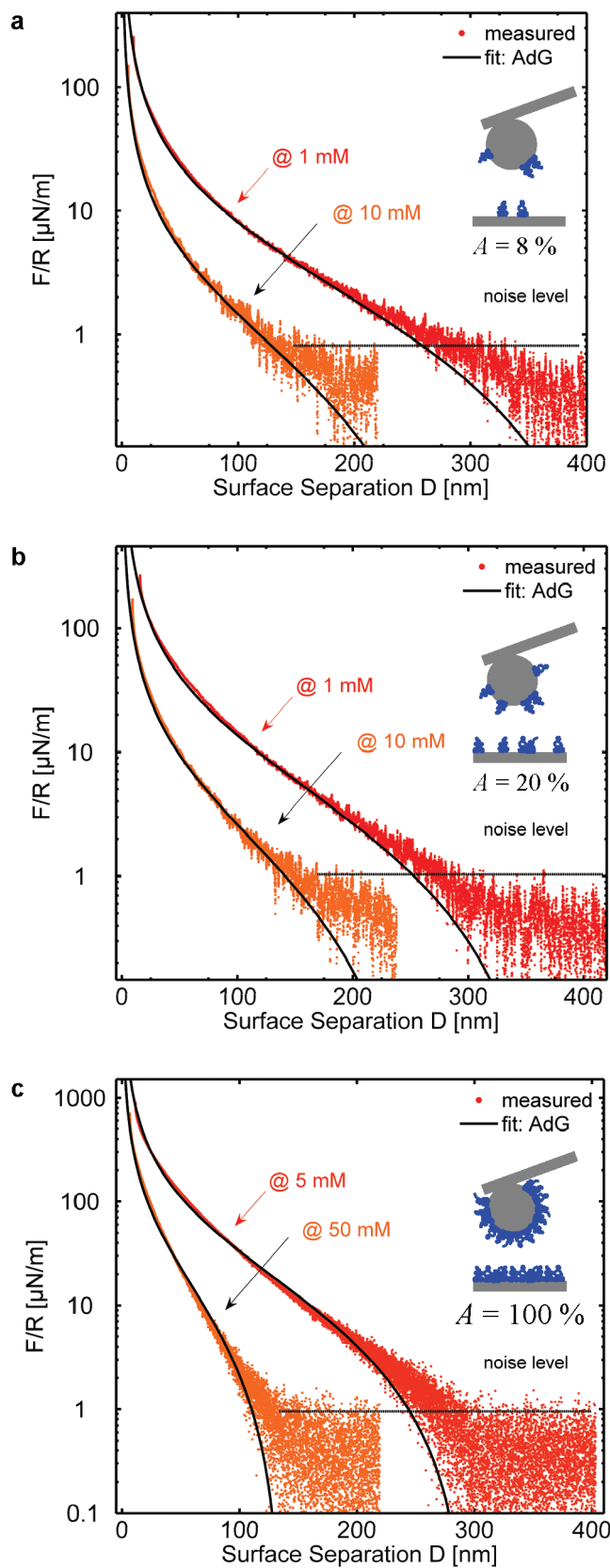


Figure 8. Representative force profiles (dots) for (a) $I_{\text{AdS}} = 0.01 \text{ M NaCl}$, (b) $I_{\text{AdS}} = 0.1 \text{ M NaCl}$, and (c) $I_{\text{AdS}} = 1 \text{ M NaCl}$, measured at a salt concentration as indicated, and the corresponding fit to eq 4 (solid line) ($N = 6800$, $v_{\text{CP}} = 0.1 \mu\text{m s}^{-1}$).

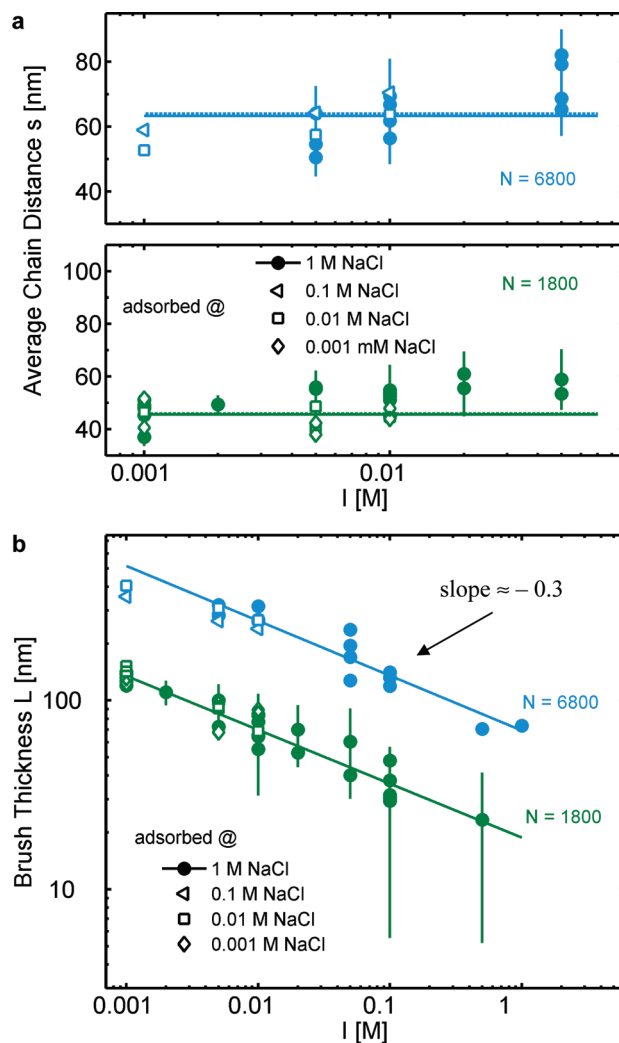


Figure 9. Average distance s between brush-like physisorbed chains (a) and brush thickness L (b), respectively, for $N = 1800$ (green) and $N = 6800$ (blue) as determined from force measurements (cf. Figures 4–8) and as function of the surrounding salt concentration. The filled symbols correspond to measurements on PSS layers physisorbed at $I_{\text{AdS}} = 1 \text{ M NaCl}$, whereas open symbols indicate lower values of the adsorption salt concentration (as indicated in the legends). One observes that the average distance s is constant during the measurements, whereas the brush thickness L shows a pronounced dependence on the bulk salt concentration I , which scales as expected for polyelectrolyte brushes.^{36,39} However, within experimental error there is no dependence of the internal properties of the brush phase (s or L) on I_{AdS} . Hence, only the area fraction A of the brush phase depends on I_{AdS} , which is a surprising and very fascinating result.

to find some intermediate states of the brush phase (for example physisorbed polyelectrolyte brushes) whose brush thickness and grafting density ($\sim s^{-2}$) is below their values at $I_{\text{AdS}} = 1 \text{ M NaCl}$. However, this is not observed here and the measurements indicate that the internal properties of the brush phase are not affected by a change in I_{AdS} .

One might consider that the fitting procedure may yield misleading results as the composed force profiles consist of many different contributions and the validity of a simple superposition is also not completely established. However, as the brush thickness L is proportional to the decay length of the steric

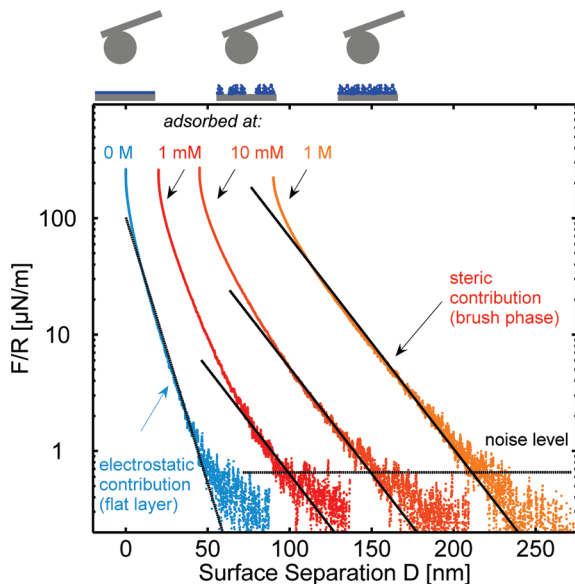


Figure 10. Asymmetric force profiles measured for $N = 1800$ at $I = 1$ mM NaCl in dependence on the salt concentration I_{AdS} in the deposition solution. To improve the clarity, the profiles are shifted with respect to the x -axis by 20 ($= 1$ mM), 40 ($= 10$ mM), and 80 nm ($= 1$ M), respectively. An increase in I_{AdS} leads to a transition of a purely electrostatic force profile ($I_{\text{AdS}} = 0$) to a purely steric one ($I_{\text{AdS}} = 1$ M NaCl). Interestingly, at intermediate I_{AdS} a biexponential decay is observed, which indicates the superposition of the electrostatic and steric contribution. Additionally, the decay length of the steric force is (within experimental error) independent on I_{AdS} , which supports the surprising observation of Figure 9 that the brush thickness L is not affected by a change in I_{AdS} .

force, it is in fact possible to show the independence of L on I_{AdS} directly in the measured force profile.

Figure 10 shows the force profiles of PSS layers physisorbed at I_{AdS} (as indicated) and measured at $I = 1$ mM NaCl. Adsorption from salt-free solution ($I_{\text{AdS}} = 0$) leads as expected to a flat PSS layer. Here, the force profile is simply described by an electrostatic repulsion and the decay length of the force profile is given by the Debye length. However, after addition of NaCl to the deposition solution ($I_{\text{AdS}} > 0$) a second contribution enters in to the force profile, which is now better described as biexponential decay. From previous measurements it is known that this long-ranged contribution is given by the steric force, created by the brush-like physisorbed PSS chains.³⁶

The strength of the steric force rises with I_{AdS} and reaches saturation for $N = 1800$ at $I_{\text{AdS}} > 0.1$ M NaCl. This makes sense, since for values of I_{AdS} exceeding 0.1 M the surface is homogeneously covered by the PSS brush phase. Both observations are in agreement with the CPTM measurements (cf. Figure 3) which indicate that the brush area fraction A (and hence the magnitude of the steric force) increases with I_{AdS} . Additionally, from the force curves one can infer that the brush thickness L is independent of I_{AdS} as the steric decay length remains constant (see solid lines in Figure 10).

Furthermore, applying the scaling law for salted polyelectrolyte brushes³³

$$L \propto N(I s^2)^{-1/3}$$

leads finally to the conclusion that also the average distance s is independent of I_{AdS} . Hence, these observations fully support the interpretation of the steric parameters of Figure 10.

Surprisingly, only the area fraction A of the brush phase depends on I_{AdS} (cf. Figure 3), which is a very fascinating result. Summarizing, one can state that a change in I_{AdS} only affects external (brush area fraction A) but not internal properties (L and s) of the brush phase. Furthermore, from the data of Figure 3 the scaling relation

$$A \propto I_{\text{AdS}}^{1/2}$$

between A and I_{AdS} is obtained. Hence, if one regards the flat and nonflat PSS domains in fact as two (thermodynamically) distinct PSS phases, then these observations lead directly to the interpretation that a change of the salt concentration I_{AdS} in the deposition solution induces a phase transition between flatly and nonflatly physisorbed PSS chains. In comparison to “more usual” phase transitions (for example condensation or transition to ferromagnetic behavior), I_{AdS} would therefore correspond to an inverse temperature of the thermodynamic system, whereas A might be interpreted as (two-dimensional) order parameter of the phase transition.⁶⁵ This analogy is further supported by the fact that an increase in I_{AdS} induces a transition from a disordered phase (the flatly physisorbed chains) into an ordered one (the brush-like physisorbed chains, which keep a quite constant distance s between them).

Please note that a similar correspondence was indeed derived by de Gennes, who noticed at first that closed self-avoiding random walks are formally described by the same equations as a certain class of ferromagnets.⁶⁶ He showed that there is an analogy between the radius of gyration of the polymer chain and the correlation length in the ferromagnet, whereby the degree of polymerization N can be understood as inverse temperature of the ferromagnet. (Thus the thermodynamic limit $N \rightarrow \infty$ corresponds to $T \rightarrow 0$ and hence always induces a phase transition, which is the crossover to ideal chain behavior for closed self-avoiding random walks.)

However, it will be interesting to see if (i) either a similar analogy can be found between brush-like physisorbed polyelectrolyte chains or (ii) if it is possible to construct some kind of Landau theory in order to describe the phase transition induced by a change in I_{AdS} . If this behavior (observed here for the special case of PSS) is indeed a real thermodynamic phase transition, then it should be a universal behavior, that is the same behavior should be observable for all linear polyelectrolytes.

Comparison of the Results with Complementary Techniques. In the previous paragraph it is argued that a change in I_{AdS} might induce a phase transition between the flat and brush-like physisorbed chains (i) as an increase in I_{AdS} generally increases the area fraction A by $A \propto (I_{\text{AdS}})^{1/2}$ and (ii) as the internal properties of the brush phase L and s (as detected by surface forces) remain unaffected upon a change in I_{AdS} .

Interestingly, using complementary techniques like UV-vis spectroscopy and neutron or X-ray reflectometry, the first property is also observed for the surface coverage Γ of single polyelectrolyte layers,^{44,49,50,52} although all these methods measure a laterally averaged surface coverage. Obviously, the surface coverage will strongly depend on the conformation of the physisorbed polyelectrolytes and it was already argued in literature, that the increase in Γ might be explained by a coiled conformation of the polyelectrolytes after deposition.⁶⁷ However, our CPTM measurements suggest that the structure of physisorbed PSS layers is formed by a coexistence of flat and brush-like physisorbed PSS chains and thus, it appears very likely

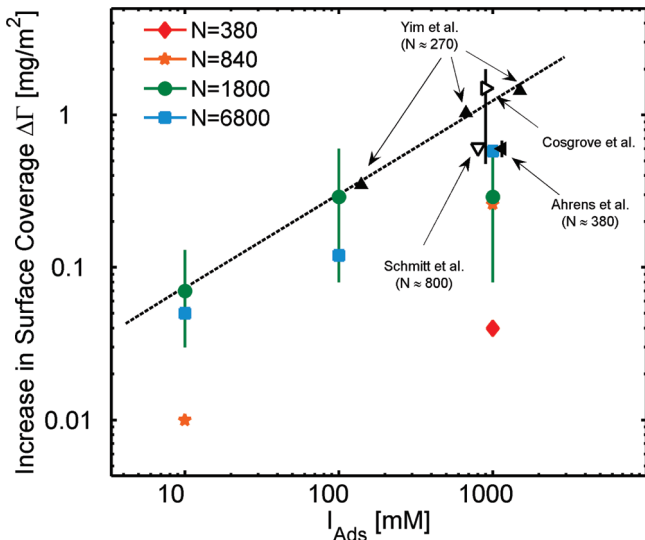


Figure 11. Increase in surface coverage $\Delta\Gamma$ (in mg/m^2) after addition of I_{AdS} salt to the deposition, obtained by a combination of CPTM and CP data (colored symbols) and by using complementary techniques as described in literature (black symbols: ∇ , Schmitt et al.; open right triangle, Cosgrove et al.; filled left triangle, Ahrens et al.; \blacktriangle , Yim et al.³²). Please note that the data points of Cosgrove, Schmitt and Ahrens refer to $I_{\text{AdS}} = 1 \text{ M NaCl}$ and have been slightly shifted horizontally (for the sake of clarity). In all references single PSS layers are investigated, which are either physisorbed to a solid substrate (cf. ∇ , Schmitt et al.⁴⁹; open right triangle, Cosgrove et al.⁴⁴) or to a liquid–air interface (cf. filled left triangle, Ahrens et al.⁵⁰; \blacktriangle , Yim et al.⁵²). Additionally, the layers are investigated using UV–vis spectroscopy (∇ Schmitt et al.⁴⁹), neutron (open right triangle, Cosgrove et al.; \blacktriangle , Yim et al.⁵²), or X-ray reflectometry (filled left triangle, Ahrens et al.⁵⁰). Interestingly, within experimental error there is a reasonable agreement between the actual work and the literature, which suggests that brush-like physisorbed PSS chains are mainly responsible for the observed increase in surface coverage. (Please refer to the text for further details on the calculation.)

that the increase in Γ upon addition of salt to the deposition solution might be given by the amount of brush-like physisorbed PSS chains.

To test this idea, it is useful to compare this amount with the increase in surface coverage, observed using laterally averaging techniques mentioned above. This is done in Figure 11, in which the increase in surface coverage $\Delta\Gamma$ (in mg/m^2) after addition of salt to the deposition solution is plotted. The data of this figure is calculated as follows:

- The black symbols are taken from the literature (as indicated in the figure), whereby the increase in surface coverage $\Delta\Gamma$ at a salt concentration I_{AdS} is defined by the difference in polyelectrolyte surface coverage Γ after deposition from a solution containing I_{AdS} and no salt: $\Delta\Gamma = \Gamma(I_{\text{AdS}}) - \Gamma$ (salt free). Hence, in this case $\Delta\Gamma$ can be interpreted as amount of polyelectrolyte, which is additionally physisorbed (compared to the salt free deposition) by addition of I_{AdS} salt to the deposition solution.
- The other symbols refer to the parameter plots of Figures 3b and 9 (and thus to direct force measurements). The surface forces (measured in this work) suggest that one brush-like physisorbed PSS chain is located in the unit volume $L s^2$. Hence, the amount of brush-like physisorbed PSS monomers per unit area is simply given by $A N / s^2$. If now m_{PSS} denotes the mass of one PSS monomer, then the mass per

unit area of nonflat physisorbed PSS monomers can be calculated using the formula

$$\Delta\Gamma(I_{\text{AdS}}) = A \cdot N \cdot m_{\text{PSS}} / s^2$$

(Please note that, although the average distance s between brush-like physisorbed chains is independent of I and I_{AdS} , it depends strongly on the degree of polymerization N . This is shown in Figure 7 of Block et al.³⁹ and Figure S1 in the Supporting Information, which serves as basis for the calculation of $\Delta\Gamma(I_{\text{AdS}})$ in the actual work.)

Interestingly, Figure 11 shows that there is a good agreement between literature data and the combination of CPTM and CP results of this work and that $\Delta\Gamma$ is generally on the order of $1 \text{ mg}/\text{m}^2$. Unfortunately, only few data is reported for low values of I_{AdS} , but for deposition salt concentrations in the molar range, a reasonable overlap of the data points is observed. This data suggests that there is a correlation between the area fraction A of the brush and the surface coverage Γ and hence that the brush-like physisorbed PSS chains might be responsible for an increase in surface coverage.

DISCUSSION

This work shows that PSS generally physisorbs in at least two phases, which differ in PSS conformation (flat versus brush domain) and in surface force (electrostatic versus steric). Using CPTM, both phases can be clearly distinguished as they create domains on the surface and thus, it is simple to determine the area fraction A of the brush-like physisorbed PSS chains. Interestingly, the area fraction A depends strongly on both the degree of polymerization N of the chains and the salt concentration I_{AdS} in the deposition solution. Furthermore, direct force measurements are used to determine the internal properties of the brush phase (the brush thickness L and the average distance s between brush-like physisorbed chains) and surprisingly, one observes that these properties are completely independent on I_{AdS} . This property and the coexistence of flatly and brush-like physisorbed PSS chains suggests that these two PSS conformations can be interpreted as two different PSS phases, whereby the ratio of both phases can be controlled by the salt concentration in the deposition solution.

The lack of influence of I_{AdS} on the PSS brush properties is a remarkable behavior, as a change in I_{AdS} is known to induce a continuous transition between a stretched (low I_{AdS}) and coiled chain conformation (high I_{AdS}) in the deposition solution and thus one would expect to find a value of L which is in between the thickness of a single, compact polyelectrolyte layer ($I_{\text{AdS}} = 0$) and the fully extended brush phase (for example at $I_{\text{AdS}} = 1 \text{ M NaCl}$). Surprisingly, this is not observed and shows clearly, that the conformation in solution does not necessarily correspond to the conformation of the adsorbed layer. For example, for $I_{\text{AdS}} = 1 \text{ mM NaCl}$ and $N = 1800$ a rather stretched conformation of PSS is observed in solution, but after adsorption almost 10% of the surface is covered by coiled and brush-like physisorbed chains (cf. Figure 3b). On the other hand, a coiled conformation is found for $I_{\text{AdS}} = 1 \text{ M NaCl}$ and $N = 380$, but after adsorption more than 90% of the surface is covered by the flat PSS phase. These examples clearly show that the surface morphology depends nontrivially on I_{AdS} and N and hence that the behavior cannot be described solely by applying the simple entropic considerations.

Additionally, it is argued in this work that the increase in surface coverage, which is usually observed after salt was added to the deposition solution, is caused to a big extend by brush-like physisorbed PSS chains. A combination of CPTM and CP data allowed to estimate the mass per unit area of the PSS brush domains which shows a reasonable agreement with literature data, obtained using complementary techniques (all of which average laterally). If further measurements are able to solidify this suggestion then this property would point to a universal behavior upon adsorption and plots similar to Figure 3b should be found generally for linear polyelectrolytes (under the appropriate deposition conditions). Additionally, a breakdown of the famous scaling $\Gamma \propto (I_{\text{Ads}})^{1/2}$ should be observed for $N > 1100$ and $I_{\text{Ads}} > 1 \text{ M NaCl}$ (as here already full surface coverage is reached). This prediction allows a test of the interpretation using complementary techniques like reflectometry or ellipsometry.

Please note, that the phase transition, which can be controlled by I_{Ads} , is frozen after adsorption, as most of the experiments indicate that there is no change in surface structure or properties if I is changed between 1 mM and 1000 mM NaCl.

For the very long PSS with $N = 6800$ some deviations from the behavior of the previous sections are observed. First of all, asymmetric and symmetric surface setups lead to force profiles, which are identical within experimental error, which is a yet unsolved problem. It is argued, that perhaps chain interdigitation might be responsible for this behavior and using the scaling relations one can calculate that the monomer concentration in the brush phases increases with decreasing N .^{33,39} Hence, an increase in N also leads to a dilution of the brush phase, which makes interdigitation more likely. However, the lack of interdigitation is also needed for a steric stabilization of adjacent (brush) chains: If opposing blobs are able to interdigitate, then this should be also possible for adjacent blobs and hence, there is no reason for the chains to adopt a brush-like conformation. In this case one would rather expect a mushroom than a polyelectrolyte brush. However, the consistency of the force profiles with previous measurements strongly suggests that the PSS chains still adopt a brush-like conformation.³⁹ Obviously, further measurements are necessary here.

OUTLOOK AND CONCLUSION

The impact of these investigations can be found in the following conclusions:

- (i) One cannot generally infer the conformation after adsorption from the chain conformation in the deposition solution. Here, additional effects (mainly monomer–monomer and monomer–substrate interactions) have to be taken into account.
- (ii) Even very low salt concentrations might lead to a noticeable amount of brush-like physisorbed PSS chains if suitable monomer substrate interactions and chain lengths are chosen.
- (iii) The increase in surface coverage Γ of single polyelectrolyte layers, $\Gamma \propto (I_{\text{Ads}})^{1/2}$, might be attributed to an increase in brush-like physisorbed PSS chains. Furthermore, homogeneous coverage of the brush phase is not self-evident.

Physisorbed polyelectrolyte layers exhibit equilibrium and nonequilibrium features: The measurements show that the basic structure of the PSS layers is not affected by changing the surrounding solution (for salt concentrations ranging between

1 mM and 1 M NaCl); the brush area fraction A and average distance s between brush-like physisorbed PSS chains are independent of the surrounding salt concentration I . This means that chains or chain parts physisorbed onto the substrate remain there. Hence, the adsorption of PSS onto the silanized silica surfaces is an irreversible nonequilibrium process. On the other hand, the brush thickness L scales reversibly as expected for a salted polyelectrolyte brush, $L \sim I^{-1/3}$, which can be understood by an equilibrium of the brush with its counterions and the bulk salt solution.³³ Hence, the brush area fraction A is an example for a nonequilibrium feature, while the thickness L of the PSS brush phase can be described by an equilibrium of the brush-like physisorbed PSS chains with the surrounding solution.

ASSOCIATED CONTENT

S Supporting Information. Figure S1 gives a short summary of all parameters plots (of the PSS brush phase), which have been derived so far and which are sufficient to describe the steric properties of the PSS brush phase. Figure S2 gives an exemplary (asymmetric) force profile obtained for $N = 6800$ and for such a large approach velocity, that an additional hydrodynamic contribution has to be regarded in the composed force profile. This material is available free of charge via the Internet at <http://pubs.acs.org>.

AUTHOR INFORMATION

Corresponding Author

*E-mail: block@physik.uni-greifswald.de. Phone: +49 3834 86-4728. Fax: +49 3834 86-4712.

ACKNOWLEDGMENT

This work was supported by the Stiftung Alfried Krupp Wissenschaftskolleg Greifswald, the BMBF (FKZ 03Z2CG1 with the ZIK HIKE project), the Deutsche Forschungsgemeinschaft (He 1616/14-1), the European Social Fund (UG 10 022) as well as the state of Mecklenburg-Vorpommern. We thank Michal Borkovec, Georg Papastavrou, Jürgen P. Rabe, and Burkhard Dünweg for helpful discussions.

REFERENCES

- (1) Decher, G. *Science* **1997**, *277*, 1232.
- (2) Caruso, F.; Caruso, R. A.; Möhwald, H. *Science* **1998**, *282*, 1111.
- (3) Yoo, P. J.; Nam, K. T.; Qi, J. F.; Lee, S. K.; Park, J.; Belcher, A. M.; Hammond, P. T. *Nat. Mater.* **2006**, *5*, 234.
- (4) Dubois, M.; Schönhoff, M.; Meister, A.; Belloni, L.; Zemb, T.; Möhwald, H. *Phys. Rev. E* **2006**, *74*, 051402.
- (5) Hiller, J.; Mendelsohn, J. D.; Rubner, M. F. *Nat. Mater.* **2002**, *1*, 59.
- (6) Netz, R. R.; Andelman, D. *Phys. Rep.* **2003**, *380*, 1.
- (7) Podgornik, R.; Ličer, M. *Curr. Opin. Colloid Interface Sci.* **2006**, *11*, 273.
- (8) Dobrynin, A. V. *Curr. Opin. Colloid Interface Sci.* **2008**, *13*, 376.
- (9) Brezesinski, G.; Möhwald, H. *Adv. Colloid Interface Sci.* **2003**, *100*, 563.
- (10) de Meijere, K.; Brezesinski, G.; Möhwald, H. *Macromolecules* **1997**, *30*, 2337.
- (11) Claesson, P. M.; Poptoshev, E.; Blomberg, E.; Dedinaite, A. *Adv. Colloid Interface Sci.* **2005**, *114*, 173.
- (12) Butt, H. J.; Cappella, B.; Kappl, M. *Surf. Sci. Rep.* **2005**, *59*, 1.
- (13) Borkovec, M.; Papastavrou, G. *Curr. Opin. Colloid Interface Sci.* **2008**, *13*, 429.

- (14) Parsegian, V. A.; Gingell, D. *Biophys. J.* **1972**, *12*, 1192.
- (15) Israelachvili, J. N. *Intermolecular and Surface forces*, 3rd ed.; Academic Press: New York, 2010.
- (16) Tabor, D.; Winterton, R. H. S. *Proc. R. Soc. London A* **1969**, *312*, 435.
- (17) Israelachvili, J. N.; Tabor, D. *Prog. Surf. Membr. Sci.* **1973**, *7*, 1.
- (18) Ducker, W. A.; Senden, T. J.; Pashley, R. M. *Langmuir* **1992**, *8*, 1831.
- (19) Meagher, L.; Pashley, R. M. *Langmuir* **1995**, *11*, 4019.
- (20) Bosio, V.; Dubreuil, F.; Bogdanovic, G.; Fery, A. *Coll. Surf. A* **2004**, *243*, 147.
- (21) Popa, I.; Gillies, G.; Papastavrou, G.; Borkovec, M. *J. Phys. Chem. B* **2009**, *113*, 8458.
- (22) Popa, I.; Gillies, G.; Papastavrou, G.; Borkovec, M. *J. Phys. Chem. B* **2010**, *114*, 3170.
- (23) Claesson, P. M.; Dahlgren, M. A. G.; Eriksson, L. *Colloids Surf. A* **1994**, *93*, 293.
- (24) Berndt, P.; Kurihara, K.; Kunitake, T. *Langmuir* **1992**, *8*, 2486.
- (25) Pericet-Camara, R.; Papastavrou, G.; Behrens, S. H.; Helm, C. A.; Borkovec, M. *J. Colloid Interface Sci.* **2006**, *296*, 496.
- (26) Lowack, K.; Helm, C. A. *Macromolecules* **1998**, *31*, 823.
- (27) Günther, J. U.; Ahrens, H.; Helm, C. A. *Langmuir* **2009**, *25*, 1500.
- (28) Borukhov, I.; Andelman, D.; Orland, H. *Macromolecules* **1998**, *31*, 1665.
- (29) Netz, R. R.; Joanny, J. F. *Macromolecules* **1999**, *32*, 9026.
- (30) Dobrynin, A. V.; Deshkovski, A.; Rubinstein, M. *Phys. Rev. Lett.* **2000**, *84*, 3101.
- (31) Dobrynin, A. V.; Deshkovski, A.; Rubinstein, M. *Macromolecules* **2001**, *34*, 3421.
- (32) Luckham, P. F.; Klein, J. J. *Chem. Soc. Faraday Trans. 1* **1984**, *80*, 865.
- (33) Zhulina, E. B.; Birshtein, T. M.; Borisov, O. V. *Macromolecules* **1995**, *28*, 1491.
- (34) Ahrens, H.; Förster, S.; Helm, C. A. *Phys. Rev. Lett.* **1998**, *81*, 4172.
- (35) Block, S.; Helm, C. A. *Phys. Rev. E* **2007**, *76*, 030801.
- (36) Block, S.; Helm, C. A. *J. Phys. Chem. B* **2008**, *112*, 9318.
- (37) de Gennes, P. G. *Macromolecules* **1980**, *13*, 1069.
- (38) de Gennes, P. G. *Adv. Colloid Interface Sci.* **1987**, *5*, 413.
- (39) Block, S.; Helm, C. A. *Macromolecules* **2009**, *42*, 6733.
- (40) Halperin, A.; Zhulina, E. B. *Langmuir* **2010**, *26*, 8933.
- (41) Fleer, G. J.; Cohen Stuart, M. A.; Scheutjens, J. M. H. M.; Cosgrove, T.; Vincent, B. *Polymers at Interfaces*; Chapman & Hall: London, 1993.
- (42) Yashiro, J.; Norisuye, T. *J. Polym. Sci. Part B* **2002**, *40*, 2728.
- (43) Adamczyk, Z.; Jachimska, B.; Jasinski, T.; Warszynski, P.; Wasilewska, M. *Colloids Surf. A* **2009**, *343*, 96.
- (44) Cosgrove, T.; Obey, T. M.; Vincent, B. *J. Colloid Interface Sci.* **1986**, *111*, 409.
- (45) Butt, H. J.; Jaschke, M. *Nanotechnology* **1995**, *6*, 1.
- (46) Sader, J. E.; Chon, J. W. M.; Mulvaney, P. *Rev. Sci. Instrum.* **1999**, *70*, 3967.
- (47) Cleveland, J. P.; Manne, S.; Bocek, D.; Hansma, P. K. *Rev. Sci. Instrum.* **1993**, *64*, 403.
- (48) Derjaguin, B. V. *Kolloid Zeits.* **1934**, *69*, 155.
- (49) Schmitt, J. Thesis, Johannes Gutenberg-Universität, Mainz, 1996.
- (50) Ahrens, H.; Baltes, H.; Schmitt, J.; Möhwald, H.; Helm, C. A. *Macromolecules* **2001**, *34*, 4504.
- (51) Gopinadhan, M.; Ivanova, O.; Ahrens, H.; Günther, J.-U.; Steitz, R.; Helm, C. A. *J. Phys. Chem. B* **2007**, *111*, 8426.
- (52) Yim, H.; Kent, M.; Matheson, A.; Ivkov, R.; Satija, S.; Majewski, J.; Smith, G. S. *Macromolecules* **2000**, *33*, 6126.
- (53) Steitz, R.; Leiner, V.; Siebrecht, R.; von Klitzing, R. *Colloids Surf. A* **2000**, *163*, 63.
- (54) Cornelisen, M.; Helm, C. A.; Block, S. *Macromolecules* **2010**, *43*, 4300.
- (55) Böhmer, M. R.; Evers, O. A.; Scheutjens, J. M. H. M. *Macromolecules* **1990**, *23*, 2288.
- (56) Hesselink, F. Th. *J. Colloid Interface Sci.* **1977**, *60*, 448.
- (57) Serr, A. Diploma Thesis, University of Geneva, Geneva, Switzerland, 2003.
- (58) Butt, H. J.; Kappl, M. *Surface and Interfacial Forces*; Wiley-VCH: Weinheim, Germany, 2010.
- (59) Alexander, S. *J. Phys. (Paris)* **1977**, *38*, 983.
- (60) O'Shea, S. J.; Welland, M. E.; Rayment, T. *Langmuir* **1993**, *9*, 1826.
- (61) Drechsler, A.; Synytska, A.; Uhlmann, P.; Elmahdy, M. M.; Stamm, M.; Kremer, F. *Langmuir* **2010**, *26*, 6400.
- (62) Israels, R.; Leermakers, F. A. M.; Fleer, G. J.; Zhulina, E. B. *Macromolecules* **1994**, *27*, 3249.
- (63) Balastre, M.; Li, F.; Schorr, P.; Yang, J. C.; Mays, J. W.; Tirrell, M. V. *Macromolecules* **2002**, *35*, 9480.
- (64) Li, F.; Balastre, M.; Schorr, P.; Argillier, J.-F.; Yang, J.; Mays, J. W.; Tirrell, M. *Langmuir* **2006**, *22*, 4084.
- (65) Stanley, H. E. *Introduction to Phase Transitions and Critical Phenomena*; Oxford University Press: New York, 1971.
- (66) de Gennes, P. G. *Scaling Concepts in Polymer Physics*; Cornell University Press: Ithaca, NY, 1979.
- (67) von Klitzing, R. *Phys. Chem. Chem. Phys.* **2006**, *8*, 5012.